CESR-c Beam Instrumentation: Bunch-by-Bunch Vertical Beam-size Monitor

William Whitaker
Physics Department, California State University-Fresno, Fresno, California, 93740
(Dated: August 8, 2003)

In an effort to better understand observed bunch-by-bunch variations at the Cornell Electron Storage Ring (CESR), an interferometer for measuring vertical beam-size on a bunch-by-bunch basis will be constructed. The first goal of this research project has been the development of software which fits the interference pattern to an equation that includes a vertical beam-size variable. This was accomplished by writing a program that minimizes a modified chi squared fit of the intensity pattern. The second goal has been to determine the viability of predicting vertical beam-size on a bunch-by-bunch basis under a variety of conditions. Results indicate that vertical beam-size can be ascertained to within 5-10% for beam-sizes ranging from 100-400 microns on a 16 turn integration. In addition, preliminary results predict that vertical beam-size measurements on a two turn integration are also possible. Furthermore, the magnification of 1.39x has been determined to provide the best accuracy in beam-size measurements for a 150 micron beam over integrations from 2-120 turns.

I. INTRODUCTION

From the generation of elementary particles to the production of high energy radiation, electron-positron accelerators have become an essential tool in scientific research. The elementary particles created from electron-positron collisions at relativistic speeds give physicists a better understanding of the universe both in the past and today. Also, the synchrotron radiation produced from electron-positron acceleration is used in medicine, crystallography, and material science research. Understanding the dynamics of electron-positron accelerators is crucial to the refinement of these invaluable tools into evermore precise, efficient machines.

In CESR, the electron and positron beams share the same beam pipe, positrons traveling in one direction, electrons traveling in the opposite direction. These two beams are electrostatically separated at all crossing points excluding the main interaction point. As the oppositely charged bunches pass in close proximity to one another, parasitic interactions can cause variations in the shape of each bunch. These differences in bunch dimensions translate into variations in luminosity between bunches at the main interaction point. The development of instrumentation which provides insight into these bunch variations could lead to significant improvements in luminosity.

With this objective in mind, an interferometer for measuring vertical beam-size on a bunch-by-bunch basis will be constructed at the Cornell Electron Storage Ring (CESR). As a preliminary study into the viability constructing such a device, this research project has focused on two specific goals. The first goal has been to develop an algorithm which fits the intensity pattern generated by the interferometer to a function containing a beam-size parameter. The second goal has been to ascertain the optimum conditions for which this algorithm provides the most accurate beam-size measurements.

In CESR, positron and electron beams are accelerated to energies in the range 1.5-5.3

GeV. During typical operating conditions, each beam consists of 9 trains of 4 or 5 bunches. Typical bunch currents are 1-10 mA, corresponding to approximately $10^{10} - 10^{11}$ electrons or positrons in each bunch. Within each train bunches are spaced at 14 ns intervals while the spacing between trains is approximately 280 ns. Angular acceleration of the bunches in the horizontal bending magnets in CESR results in the emission of synchrotron radiation in the plane of the accelerator ring. This synchrotron radiation can be used to image the transverse shape of the beam which is an ellipse with its minor axis oriented vertically. Vertical beam-size is of particular interest and can be described by a Gaussian profile (see Fig. 1).

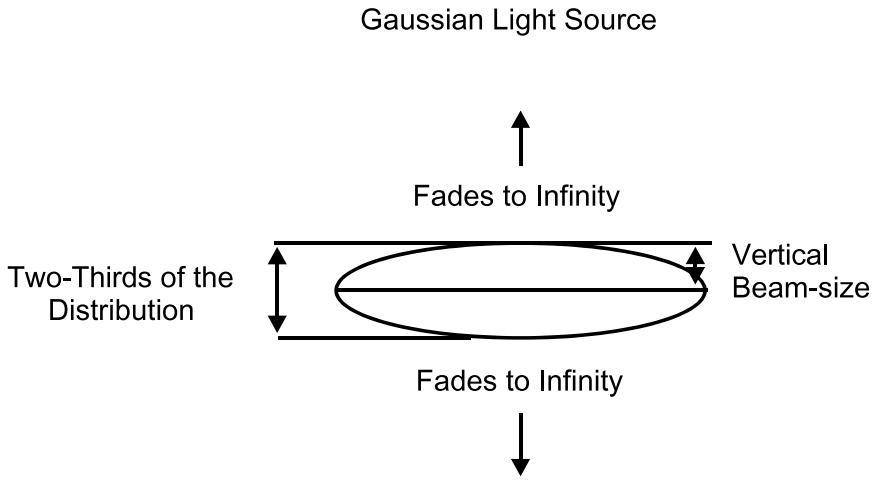

FIG. 1: Vertical beam-size measurement of Gaussian source

When flashes of synchrotron light from the beam are projected onto a charge couple device (CCD), the relatively slow response time of the CCD integrates the synchrotron radiation from all the bunches over many revolutions of the machine. Presently, this is the way in which beam-size is measured. With the advent of affordable photomultiplier tube (PMT) linear arrays, a means for measuring vertical beam-size on a bunch-by-bunch basis is readily available. Hamamatsu Photonics is producing a Multianode PMT Assembly which sells for around $2000. This device has thirty-two channels, each with a response time of 0.6 ns, spaced 1 mm apart. The combination of affordability and speed, packaged in a linear array with the spatial orientation capable of resolving the light source pattern, is the breakthrough needed to make beam-size comparisons between bunches.

To accomplish the task of making vertical beam-size measurements, an interferometer, using double slit diffraction, will be setup in CESR. The broad spectrum of synchrotron radiation from individual bunches will be filtered to produce a quasi-monochromatic source. The filtered light will pass through two narrow, closely spaced slits, and the resulting diffraction pattern will project onto a 32 channel PMT (see Fig.2). The intensity at the PMT can be described by the equation:

$$I(x) = I_0 \left[\frac{\sin(\frac{2\,\pi\,w\,x}{f\,\lambda})}{\frac{2\,\pi\,w\,x}{f\,\lambda}} \right]^2 \left[1 + V\,\cos\left(\frac{2\,\pi\,d\,x}{f\,\lambda} \right) \right] \tag{1}$$

where, w=slit width, d=slit spacing, f=focal length of the lens, λ=wavelength of quasi-monochromatic light, and x= displacement along the PMT. V is the visibility of the fringes

and can be derived from the Fourier transform of the normalized angular distribution function of the light source [1]. After conversion from angular distribution to linear displacement, the visibility is described by the equation:

$$V = e^{-2\left(\frac{\pi\, d\, \sigma_{beam}}{L\,\lambda}\right)^2} \tag{2}$$

where, L is the distance from source to slits, and σ_{beam} is the vertical beam sigma of the Gaussian shaped light source (beam-size). The other variables are as previously described. (For the prototype interferometer the purposed specifications are: L=5m, λ=500nm, w=250μm, d=2mm, and f=0.3m)

As the diffraction pattern strikes the PMT, a current proportional to the intensity is generated in each channel. This signal is amplified, converted to a voltage, and then digitized by an analog-to-digital converter (ADC). The ADC outputs from all 32 channels will then be fitted to the intensity function with a digital signal processor (DSP). Beam-size will then be derived from the visibility function.

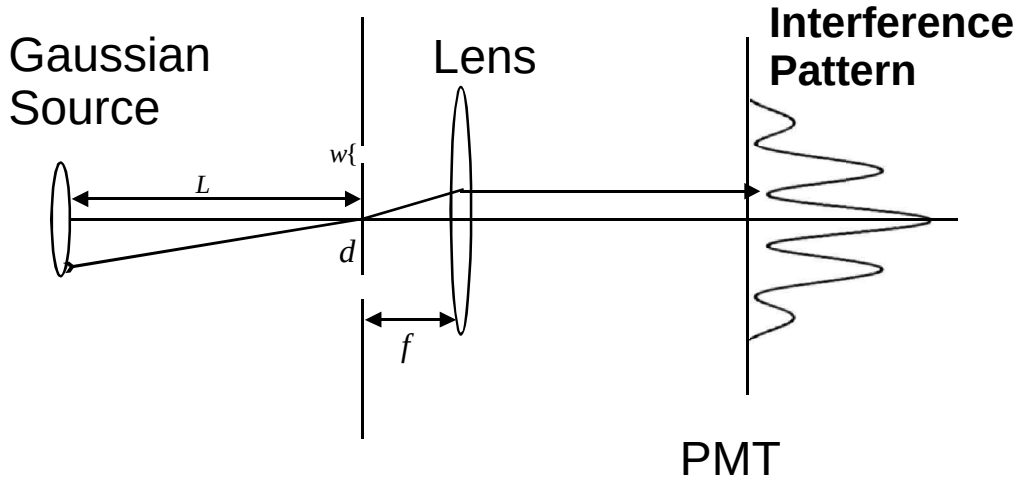

FIG. 2: Double Slit Diffraction: L=distance from source to slits, w=slit width, d=slit spacing, f=focal length of the lens

Determining the magnification of the diffraction pattern (i.e. the portion of the diffraction pattern to be sampled) is of particular importance for the construction of the interferometer. Projection of the intensity pattern onto the 32 channel PMT produces very few data points with which to fit the intensity function (see Fig. 3). By increasing the magnification (imaging a smaller portion of the pattern), the same number of data points cover a smaller area, making that portion of the pattern more discernible (see Fig. 4). However, if too small a section of the diffraction pattern is sampled at the PMT, not enough of the fringes will be included to determine visibility or, as follows, vertical beam-size. Therefore, the challenge is to find the point at which the portion of the pattern is small enough to resolve the shape of the waveform but not so small that fringe information is lost. Furthermore, as the magnification increases, intensity decreases. Ultimately, determining beam-size on a one or two turn basis would be an ideal objective. Increasing magnification reduces the viability of this option by further reducing the already sparse number of photons available (see Fig. 5).

So, increases in magnification need to leave enough photons to facilitate 1-2 turn vertical beam-size measurements.

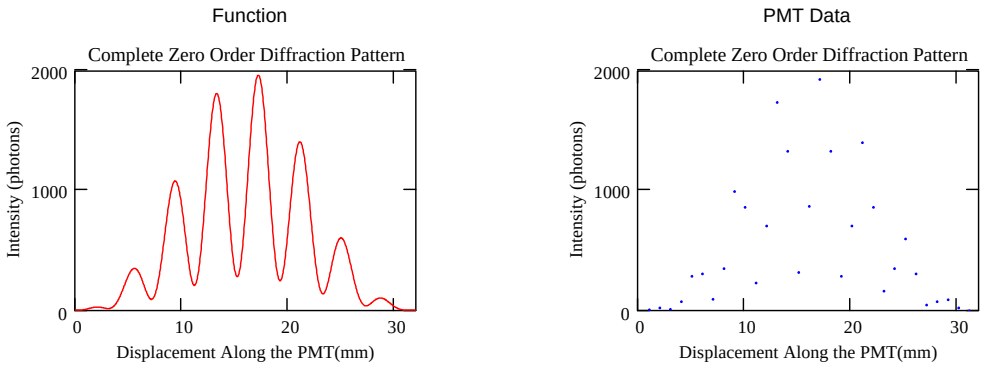

FIG. 3: Simulated data for a 1.00x magnification of the zero order diffraction pattern integrated over 16 turns

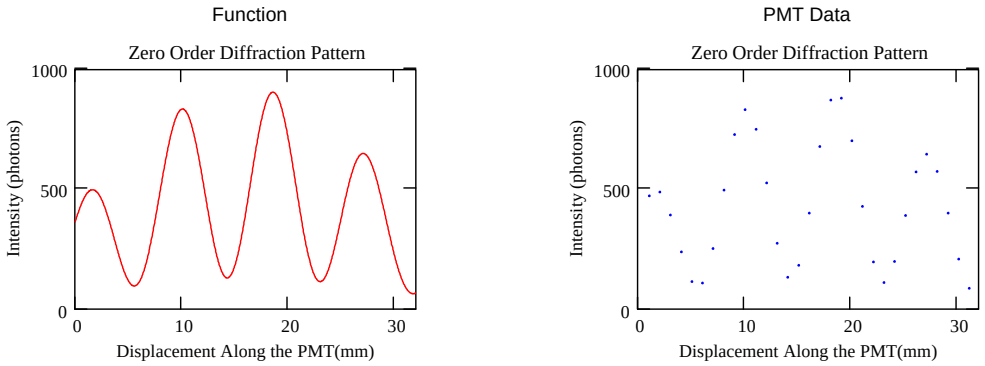

FIG. 4: Simulated data for a 2.17x magnification of zero order diffraction pattern integrated over 16 turns

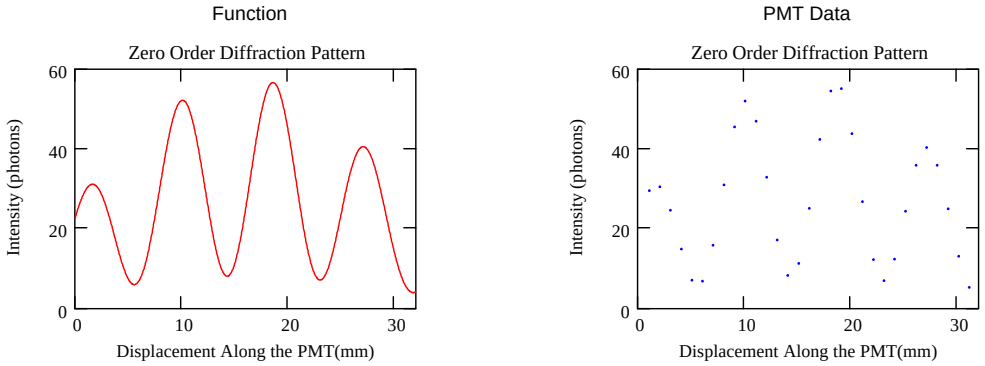

FIG. 5: Simulated data for a 2.17x magnification of zero order diffraction pattern integrated over 1 turn

II. METHODS

The first objective of this research project has been to write a program which fits data generated by a 32 channel PMT to the functional form of the intensity pattern as given in Equation 1. The second objective has been the use of that fitting program to determine the magnification of the diffraction pattern which yields the best fit to the function. Also, the program must perform the fit quickly. As stated above, it will run in a DSP, which does not have the resources of a PC. The results of this research will then be used in ascertaining optimum specifications for optics in the interferometer.

A fitting program was written in *C* programming language to minimize the chi squared fit of the parameterized function for intensity. First, the individual constants at each parameter were consolidated into one parameter. For example, $\frac{2\pi w}{f\lambda}$ became a_2. Next, an x-axis translation was introduced into the equation. This parameter (a_3) accounts for the fact that the interference pattern will be centered at some point other than at zero. Finally, a phase offset (a_6) was introduced. Phase offsets in the fringes arise from slight misalignments of the light source, lens or slits in the interferometer. With the phase offset and x-axis translation, the intensity function is given by the following equation:

$$I(x) = a_1 \left[\frac{\sin(a_2 x - a_3)}{a_2 x - a_3}\right]^2 [1 + a_4 \cos(a_5 x - a_6)] \tag{3}$$

And the χ^2 function is given by:

$$\chi^2 = \sum_{i=1}^{n} \left[\frac{(y_i - I(x_i))}{\sigma_i}\right]^2 \tag{4}$$

where the summation is the sum of the 32 data points generated by the PMT and σ_i is the variance at each point. If, for the purpose of simplifying the fitting function, we assume that the variance at each point is uniform, ${\sigma_i}^2$ can be moved to left side of the equation. The minimization is, then, actually performed on ${\sigma_{SD}}^2\chi^2$ and is given by the equation:

$${\sigma_{SD}}^2\chi^2 = \sum_{i=1}^{n} [y_i - I(x_i)]^2 \tag{5}$$

In the limit of fitting data from only a few turns, this assumption will not be rigorously true due to the Poisson statistics inherent in the data. However, the idea is that fits are made more quickly with fewer parameters in the fitting algorithm. The hope is that the program will return the other parameter values with a degree of precision accurate enough to preclude an explicit declaration of variance for each point in the fitting algorithm. Fortunately, the assumption has been correct.

The fitting program minimizes the modified chi squared function by calling two subroutines presented in *Numerical Recipes in C*. The first is frprmn.c which uses the Polak-Ribiere variant to minimize each of the parameters in the chi square function. This is accomplished in part with the second *NR* subroutine dfridr.c, which finds the derivative of the chi squared function at particular points, using Ridder's method [2].

When given a data set and "best guess" set of parameters, the program will return the fitted parameters and the number of iterations to convergence. Smaller iteration values are indicative of quick convergence.

The first step in determining the robustness of the program was to generate data using Equation 3. The x-axis translation mentioned earlier was scaled to mimic the projection of the intensity pattern onto the center of the 32 channel PMT. I_0 values (a_1 in Eq. 3) were scaled to reflect intensity in terms of the number of photoelectrons detected at each channel, based on data gathered though previous experiments (where L=5m, λ=500nm, w=250μm, d=2mm, and f=0.3m). For one turn of one bunch, approximately 100 photo electrons are contained in the center 20% of the middle fringe.

Secondly, errors were imposed to reflect the limitations of the device. First, a counting error was imposed by giving generated intensities a Poisson distribution. Next, this altered intensity was given a 0-3.6% Gaussian distribution error to simulate a systematic gain error peculiar to the PMT. Lastly, a 1% flat error was added to account for noise generated as the signal is processed in the ADC.

Finally, a series of fits were performed on generated data with errors as described above. Magnifications were varied from 1.00x to 2.17x in an effort to determine the optimum portion of the the diffraction pattern with which to work. Figure 6 gives a graphical representation for the various magnifications used in the fits. Additionally, intensities were varied to reflect integrations of light from one bunch for 2 to 120 turns around CESR. This latter variation gave insight into the viability of measuring vertical beam-size on a few turn basis. To determine the robustness of the fitting routine over a variety of beam-sizes, vertical beam-sizes were varied from 100 to 400 microns. However, due to time constraints the majority of the research has been conducted with a beam-size of 150 microns.

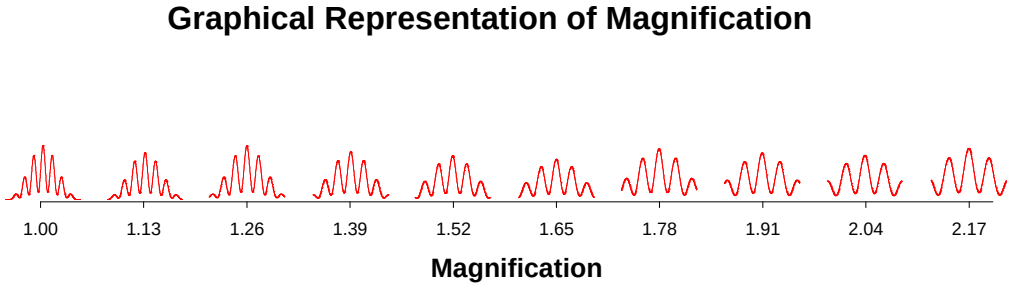

FIG. 6: Portions of the intensity pattern observed at the PMT with various magnifications

III. RESULTS

Figure 7 shows the routine's performance in fitting a 150 micron bunch with 2-120 turn integrations. The fractional error begins to level off around 12-16 turns. A 16 turn integration is also where fit failures go to zero (see Tab. I) and fitting is reasonably uniform for all magnifications. For these reasons, a 16 turn integration is a good place to begin exploring the program's behavior.

To get a feel for how the fractional error in determining vertical beam-size varies with visibility, let us revisit Equation 2. A little calculus and algebra will yield the relationship:

$$\frac{\Delta\sigma}{\sigma} = \frac{\Delta V}{V}\frac{1}{2lnV} \tag{6}$$

Using 16 turn integrations, the program fits with a RMS of ΔV at 0.027 for visibilities

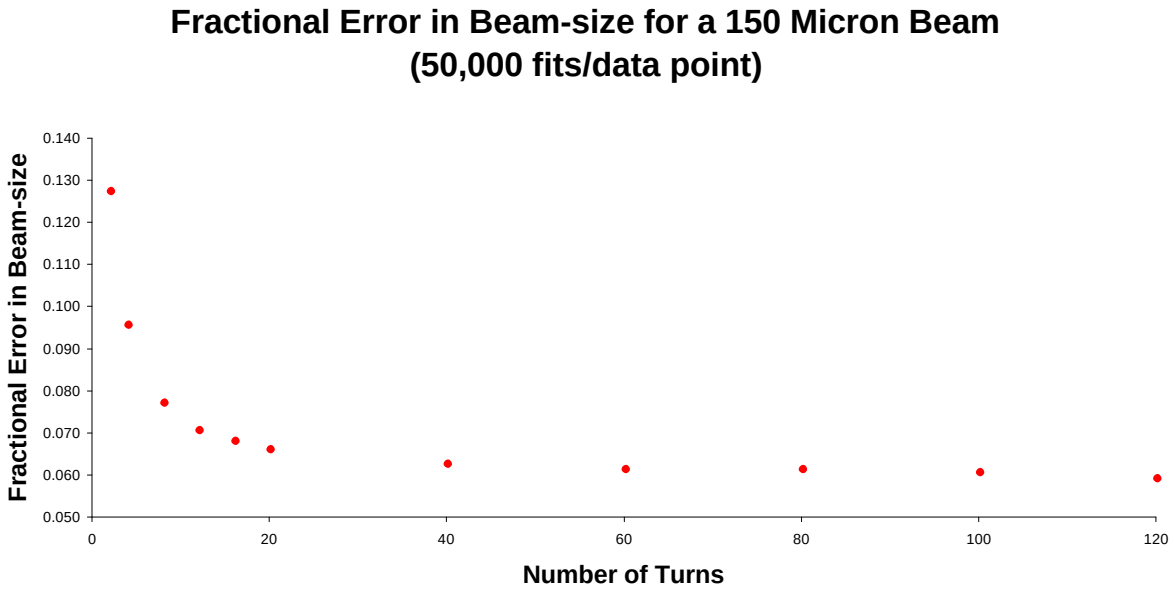

FIG. 7: RMS of Fractional Error in Beam-size

ranging from 0.17-0.75. With this value in Equation 6, Figure 8 shows the limits for resolving vertical beam-size as the visibility changes.

After calculating beam sigma from visibility, the solid line in Figure 9 shows the fractional error in beam-size versus beam-size. When several sets of 50,000 fits are added to the graph, the robustness of the program is readily apparent. The results are in excellent agreement with predictions, determining beam-size with about 93% accuracy for a 150 micron beam. In addition the percentage of failures in this region is essentially zero (Tab. II). In fact, the percentage of fit failures is reasonably small for all the beam-sizes tested in the range. When the routine is implemented in a working interferometer, a failed fit will simply be identified and a new integration will be taken.

With regard to the prospect of determining beam-size on a two turn integration, for a 150 micron beam, the fitting program continued to work quite well. However, accuracy drops approximately 3% for magnifications ranging from 1.00x to 1.65x (see Fig. 10). For

TABLE I: Fit Failure Rates for 2-16 Turns Integrations: 5000 Fits/Magnification

Magnification	2 Turns	4 Turns	8 Turns	12 Turns	16 Turns
1.00x	0.00%	0.00%	0.00%	0.00%	0.00%
1.13x	0.02%	0.00%	0.00%	0.00%	0.00%
1.26x	0.02%	0.00%	0.00%	0.00%	0.00%
1.39x	0.02%	0.00%	0.00%	0.00%	0.00%
1.52x	0.06%	0.00%	0.00%	0.00%	0.00%
1.65x	0.00%	0.00%	0.00%	0.00%	0.00%
1.78x	0.14%	0.00%	0.00%	0.00%	0.00%
1.91x	0.34%	0.08%	0.02%	0.00%	0.00%
2.04x	0.58%	0.12%	0.00%	0.00%	0.00%
2.17x	1.50%	0.42%	0.04%	0.02%	0.00%

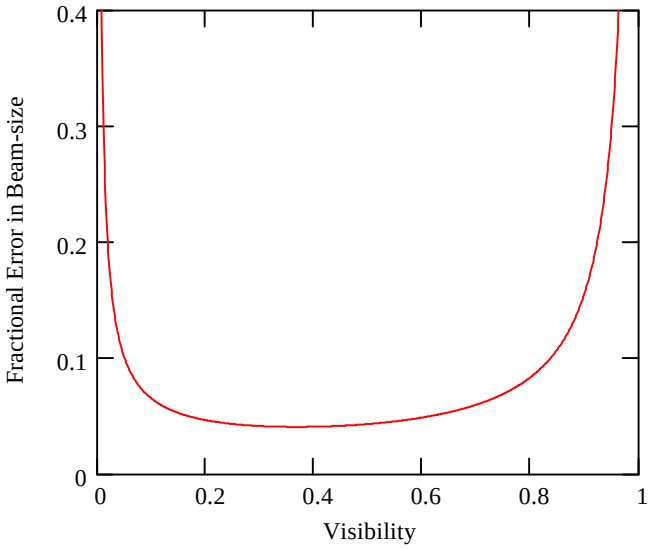

FIG. 8: Fractional Error in determining beam-size versus visibility for 16 turn integrations

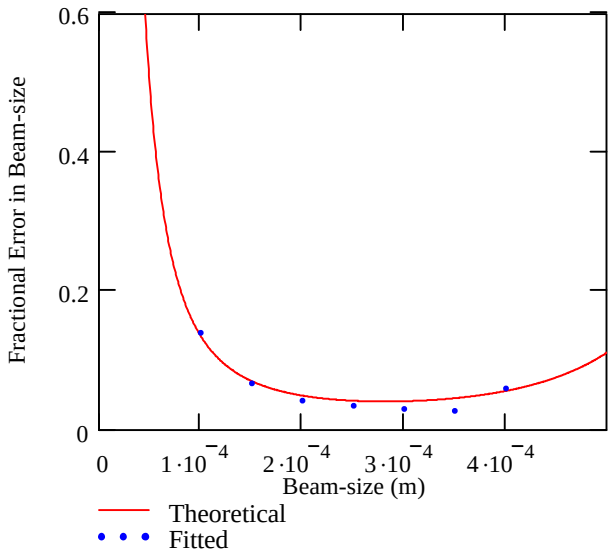

FIG. 9: Fractional Error in determining beam-size versus beam-size for 16 turn integrations

magnifications greater than 1.65x accuracy begins to drop rapidly. In addition, as reflected in Table III, the failure rates start increasing at 1.78x. When vertical beam-size is increased to 325 microns, the accuracy increases to about 95% (see Fig. 11). This result is reasonable; as beam-size increases visibility decreases, which equates to greater intensity at the bottom of the fringes. Greater intensity at the bottom of the fringes, just as with the 16 turn case, means a more accurate fit. However, failure rates also increase (Tab. II). The increase in failure rates at greater magnifications is likely due to the program's inability to resolve the fringes with the reduced visibility and only 32 data points.

Finally for a 150 micron beam, a magnification of 1.39x provides the best accuracy in beam-size measurements. Fits performed at this magnification have the most uniform distribution for integrations ranging from 2-120 turns (see Fig. 12). Furthermore, at 1.39x magnification the program experiences only one fit failure at a two turn integration.

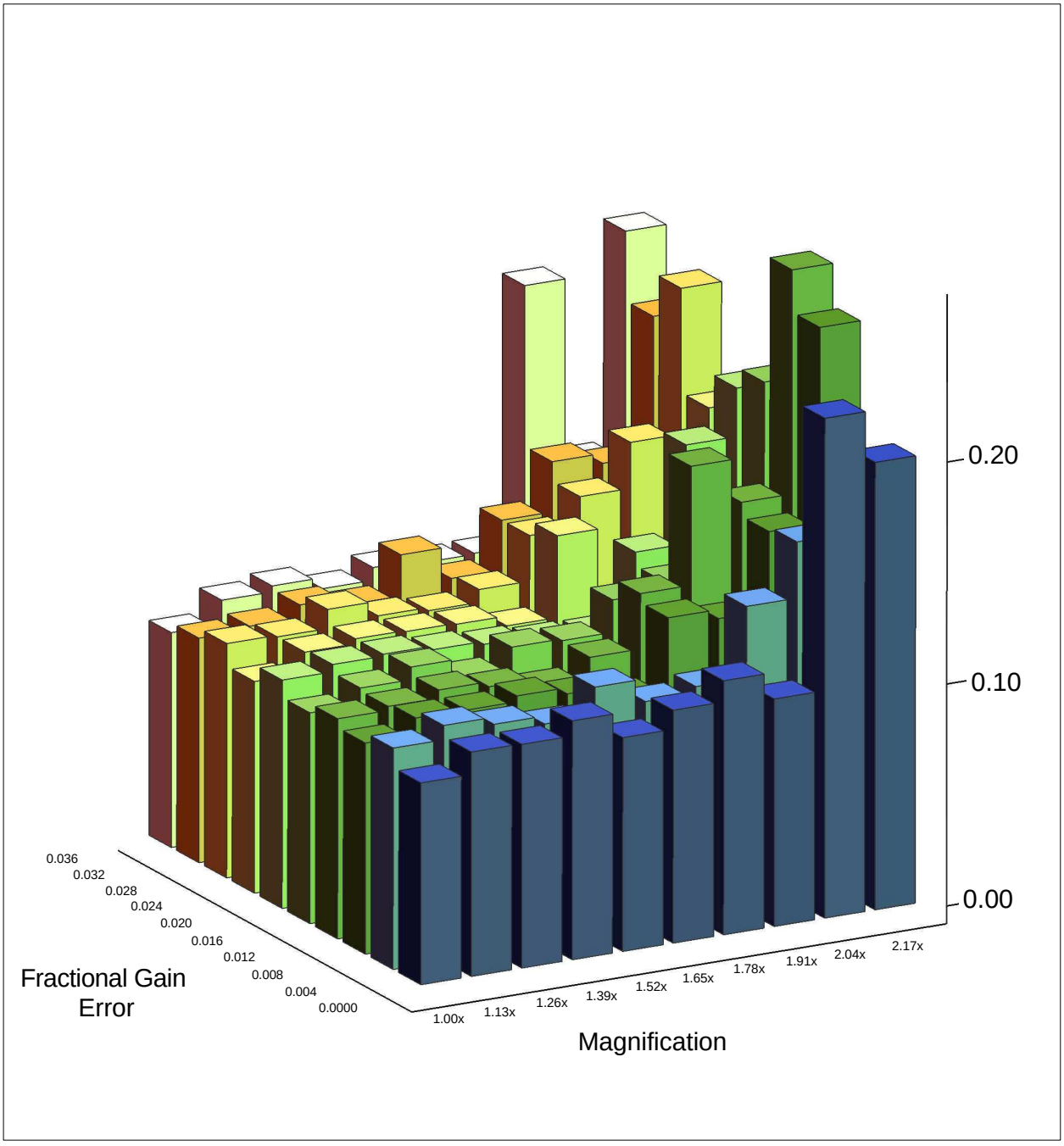

M

FIG. 10: The vertical axis gives the RMS of fractional error in beam-size measurements as a function of magnification and gain error. The fits were made on data simulating a 150μm beam integrated over two turns. (fit failures as presented in Table III were excluded)

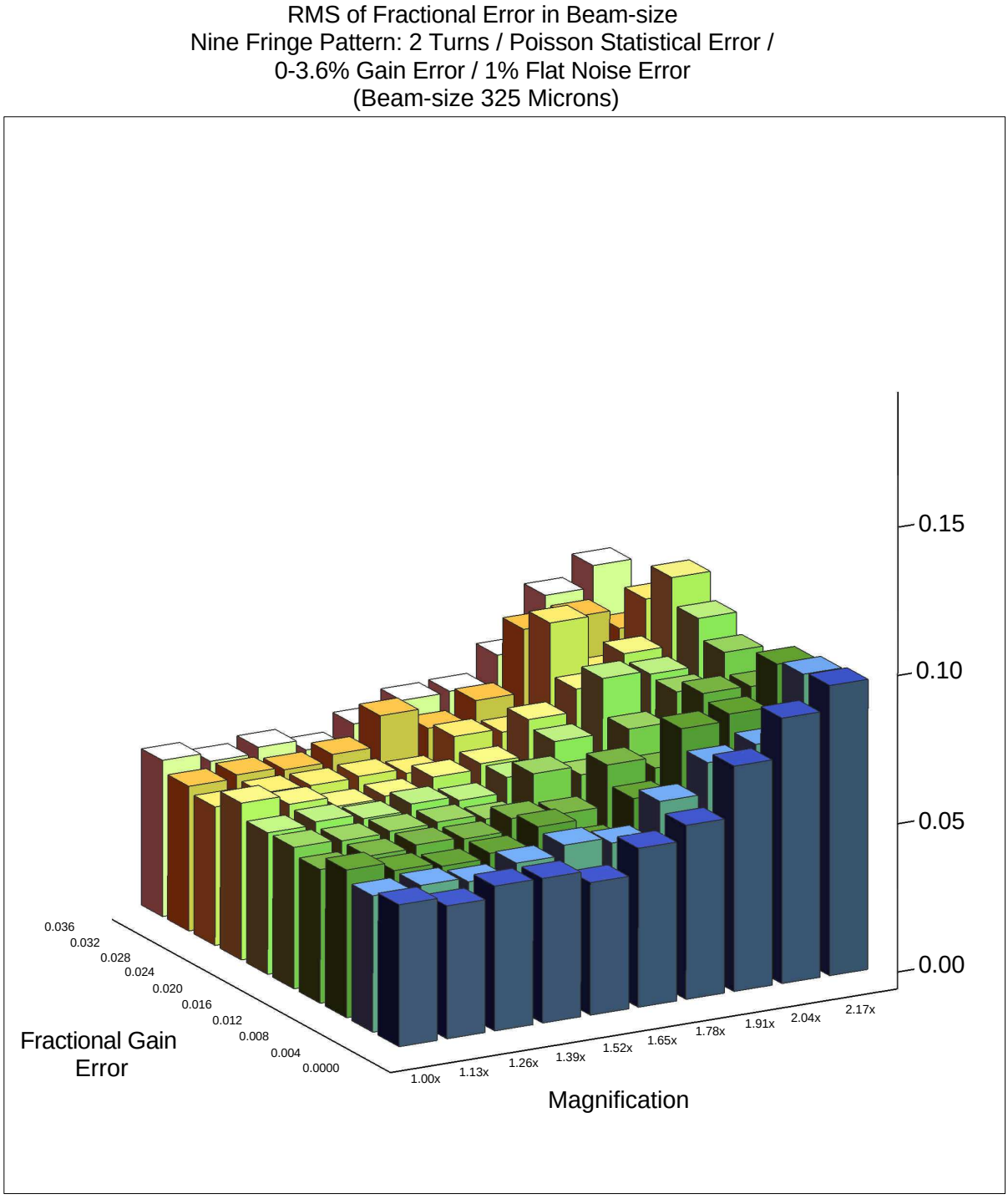

M

FIG. 11: The vertical axis gives the RMS of fractional error in beam-size measurements as a function of magnification and gain error. The fits were made on data simulating a 325μm beam integrated over two turns. (fit failures as presented in Table III were excluded)

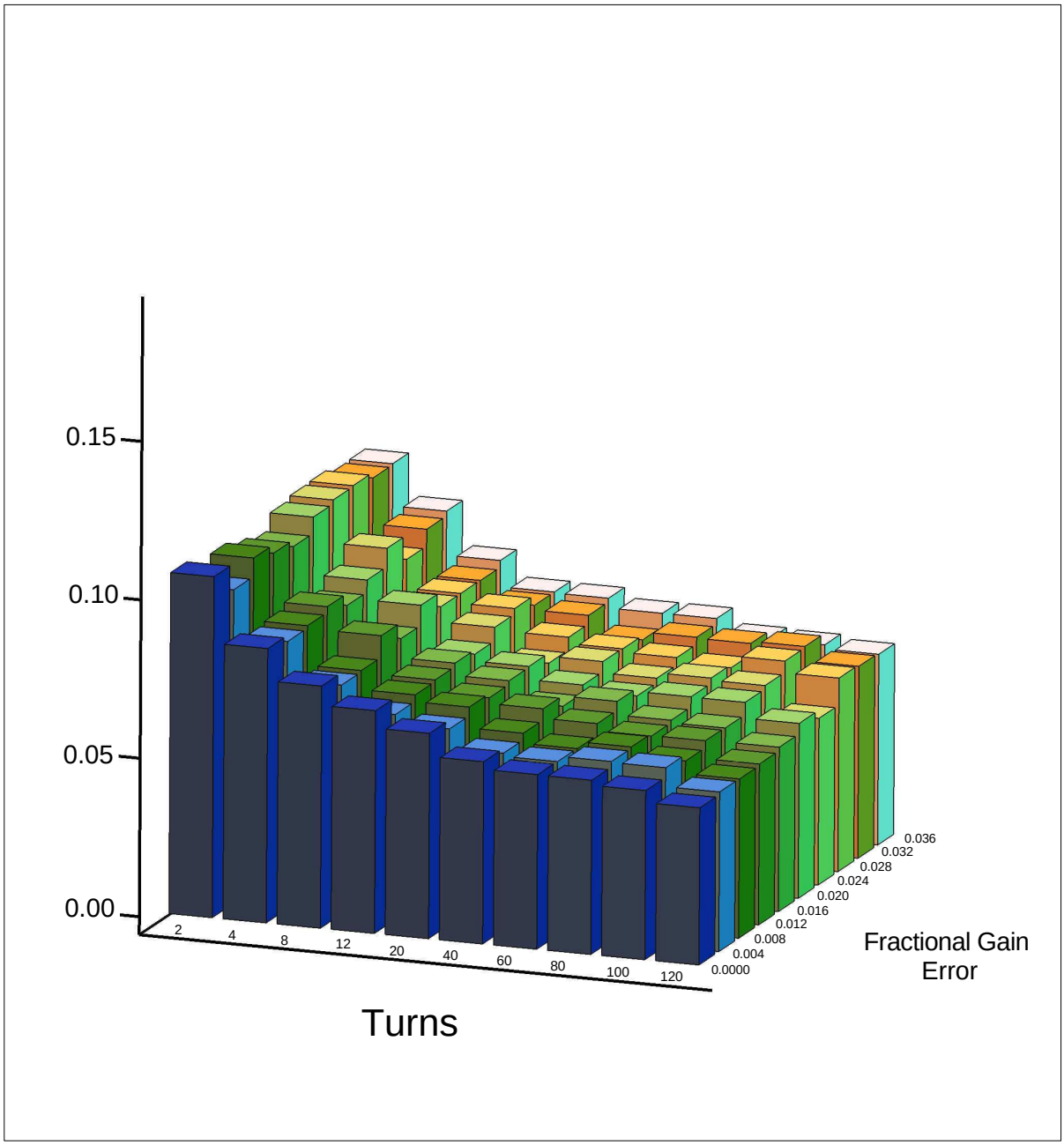

M

FIG. 12: The vertical axis gives the RMS of fractional error in beam-size measurements as a function of turns of integration and fractional gain error. The fits were made on data simulating a 150μm beam with a 1.39x magnification of the diffraction pattern.

TABLE II: Fit Failure Rates for 16 Turn Integrations: 50,000 Fits/Beam-size

Bunch-size	Percent Error in Determining Beam-size	Failure Rate
100μm	13.97%	0.002%
150μm	6.74%	0.000%
200μm	4.24%	0.002%
250μm	3.48%	0.01%
300μm	2.98%	0.09%
350μm	2.75%	0.44%
400μm	5.93%	1.54%

TABLE III: Fit Failure Rates for 2 Turn Integrations: 5000 Fits/Magnification

Magnification	150μm Beam-size	325μm Beam-size
1.00x	0.00%	0.02%
1.13x	0.02%	0.08%
1.26x	0.02%	0.04%
1.39x	0.02%	0.24%
1.52x	0.06%	0.48%
1.65x	0.00%	1.18%
1.78x	0.14%	2.70%
1.91x	0.34%	4.96%
2.04x	0.58%	7.96%
2.17x	1.50%	10.28%

Unfortunately, time constraints prohibited extensive evaluation of the impact of magnification on the program's performance. Although the effects of magnification were examined in detail for a 150 micron beam, additional data analysis is required for for beam-sizes between 100-400 microns.

IV. ACKNOWLEDGMENTS

Special thanks to Mark Palmer-Cornell University, Rich Galik-Cornell University, and the National Science Foundation for providing me with the opportunity to succeed. I'd also like to thank the other REU students for a memorable summer.

This work was supported by the National Science Foundation REU grant PHY-0101649 and research co-operative agreement PHY-9809799.

[1] M. Klein, *Optics*, 257-270, Wiley: New York, (1970)

[2] William H. Press, et al., *Numerical Recipes in C*, 186-189 and 420-425, CUP: Cambridge, (1992)